Discovery of Potent & Selective Inhibitors of Activated Thrombin-Activatable Fibrinolysis Inhibitor for the Treatment of Thrombosis

Mark E. Bunnage,*,[†] Julian Blagg,[†] John Steele,[†] Dafydd R. Owen,[†] Charlotte Allerton,[†] Andrew B. McElroy,[†] Duncan Miller,[†] Tracy Ringer,[†] Ken Butcher,[†] Kevin Beaumont,[‡] Karen Evans,[‡] Andrew J. Gray,[§] Stephen J. Holland,[§] Neil Feeder,[#] Robert S. Moore,[⊥] and David G. Brown[⊥]

Pfizer Global Research and Development, Sandwich Laboratories, Ramsgate Road, Kent CT13 9NJ, U.K.

Thrombin-activatable fibrinolysis inhibitor (TAFI) has emerged as a key link between the coagulation and fibrinolysis cascades and represents a promising new target for the treatment of thrombosis. A novel series of imidazolepropionic acids has been designed that exhibit high potency against activated TAFI (TAFIa) and excellent selectivity over plasma carboxypeptidase N (CPN). Structure activity relationships suggest that the imidazole moiety plays a key role in binding to the catalytic zinc of TAFIa, and this has been supported by crystallographic studies using porcine pancreatic carboxypeptidase B as a surrogate for TAFIa. The SAR program led to the identification of **21** (TAFIa Ki = 10 nM, selectivity TAFIa/CPN > 1000) as a candidate for clinical development. Compound **21** exhibited antithrombotic efficacy in a rabbit model of venous thrombosis, yet had no effect on surgical bleeding in the rabbit. In addition, **21** exhibited an excellent preclinical and clinical pharmacokinetic profile, characterized by paracellular absorption, low clearance, and a low volume of distribution, fully consistent with its physicochemical properties of low molecular weight (MW = 239) and high hydrophilicity (log D = −2.8). These data indicate **21** (UK-396,082) has potential as a novel TAFIa inhibitor for the treatment of thrombosis and other fibrin-dependent diseases in humans.

Introduction

Thrombotic diseases are among the more common causes of mortality and morbidity in the developed world. A number of agents are available for the treatment and prevention of thrombotic disease, but these are generally anti-coagulants with significant drawbacks, including varying degrees of adverse hemorrhagic side-effects. Heparin and low-molecular-weight heparins are administered parenterally and are thus generally used as short-term treatments only. Chronic oral antithrombotic therapy is centered on the use of warfarin, which requires regular patient monitoring because of its significant safety liabilities, including severe adverse bleeding events and significant drug–drug interactions. Overall, there remains a clear medical need for new antithrombotic agents that are safer than established therapies and are suitable for chronic oral administration.

Activation of the coagulation cascade leads ultimately to thrombus formation through the generation of thrombin and the subsequent conversion of soluble fibrinogen to fibrin. Fibrin polymerizes to form an insoluble matrix that acts as an essential scaffold for the developing thrombus. Fibrin is regulated by the balance between its synthesis via the coagulation cascade and its clearance via the fibrinolysis cascade. Fibrinolysis results from the generation of plasmin, a serine protease that breaks down fibrin to soluble fibrin degradation products (FDPs),[a] ultimately leading to dissolution of the thrombus. The pharmaceutical industry has devoted considerable effort to the discovery of potential new antithrombotic agents that act on the coagulation cascade, particularly inhibitors of thrombin and factor Xa. Until recently, very little attention has been devoted to agents that can enhance fibrinolysis.

Thrombin-activatable fibrinolysis inhibitor (TAFI)[1,2] is a 60-kDa glycoprotein zymogen found in human plasma.[3] Thrombin has been shown to convert TAFI from the inactive zymogen to its activated form (TAFIa), a proteolytic cleavage reaction that is significantly augmented by thrombomodulin. TAFIa (also known as plasma carboxypeptidase B[4] and carboxypeptidase U[5]) is an unstable basic carboxypeptidase that has been found to significantly inhibit endogenous fibrinolysis, and TAFI has thus emerged as the molecular link between the coagulation and fibrinolysis cascades.[3,6] It is believed that the inhibition of fibrinolysis by TAFIa is due to its ability to down-regulate the formation of plasmin. Plasmin is generated from the zymogen plasminogen by the action of tissue-type plasminogen activator (*t*-PA). Both *t*-PA and plasminogen contain kringle domains that recognize key C-terminal lysine residues on fibrin and aid the formation of a ternary complex between *t*-PA, plasminogen, and fibrin that is believed to be critical to the generation of plasmin at the site of a thrombus. In addition, cleavage of fibrin to the FDPs by plasmin results in exposure of new C-terminal lysine residues, thereby amplifying the generation of plasmin and further enhancing clot lysis. TAFIa is implicated in the removal of the C-terminal lysine residues from both fibrin and FDPs, thereby inhibiting plasmin generation and reducing fibrinolysis. Consequently, *inhibition* of TAFIa has the potential to *enhance* endogenous fibrinolysis and thus represents an

---

* To whom correspondence should be addressed. Address: Pfizer Global Research and Development, Sandwich Laboratories, ipc 432, Ramsgate Road, Kent CT13 9NJ, U.K. Tel: +44 1304 648974. Fax: +44 1304 651987. E-mail: mark.bunnage@pfizer.com.
[†] Department of Discovery Chemistry.
[‡] Department of Pharmacokinetics, Dynamics & Metabolism.
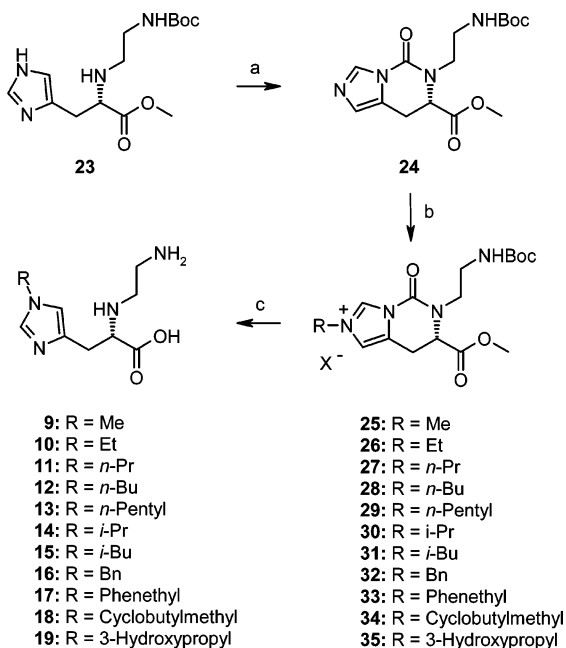[§] Department of Discovery Biology.
[#] Department of Pharmaceutical Sciences.
[⊥] Department of Structural Biology.

[a] Abbreviations: FDPs, fibrin degradation products; TAFI, thrombin-activatable fibrinolysis inhibitor; TAFIa, activated thrombin-activatable fibrinolysis inhibitor; *t*-PA, tissue-type plasminogen activator; CPA, bovine pancreatic carboxypeptidase A; ACE, angiotensin-converting enzyme; pCPB, pancreatic carboxypeptidase B; CPN, human plasma carboxypeptidase N; GFR, glomerular filtration rate.

Scheme 1[a]

[a] Reagents: (a) NaOAc, *tert*-butyl *N*-(2-oxoethyl)carbamate, NaCNBH$_3$, 4 Å molecular sieves (b) i, TFA, MeOH, H$_2$O; ii, aq. NaOH; iii, Dowex 50WX8-200.
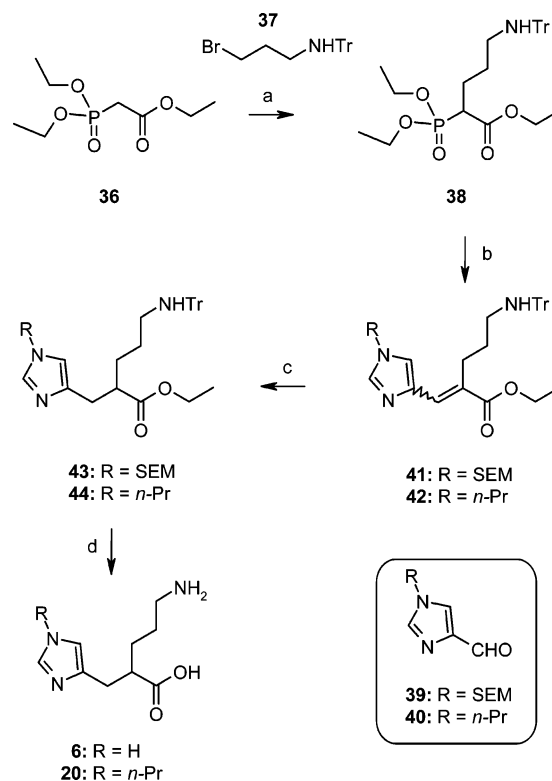
Scheme 2[a]

9: R = Me	**25:** R = Me
10: R = Et	**26:** R = Et
11: R = *n*-Pr	**27:** R = *n*-Pr
12: R = *n*-Bu	**28:** R = *n*-Bu
13: R = *n*-Pentyl	**29:** R = *n*-Pentyl
14: R = *i*-Pr	**30:** R = *i*-Pr
15: R = *i*-Bu	**31:** R = *i*-Bu
16: R = Bn	**32:** R = Bn
17: R = Phenethyl	**33:** R = Phenethyl
18: R = Cyclobutylmethyl	**34:** R = Cyclobutylmethyl
19: R = 3-Hydroxypropyl	**35:** R = 3-Hydroxypropyl

[a] Reagents: (a) carbonyldiimidazole, DMF; (b) RX (X = Br or I), CH$_3$CN; (c) i, concd HCl or H$_2$SO$_4$; ii, Dowex 50WX8-200.

Scheme 3[a]

[a] Reagents: (a) i, NaH, THF; ii, *N*-(3-bromopropyl)-*N*-tritylamine **37**, 18-crown-6; (b) i, NaH, THF; ii, aldehyde **39** or **40**; (c) Pd/C, H$_2$, EtOH (R = SEM) *or* NaBH$_4$, CuCl, MeOH (R = *n*-Pr); (d) i, aq. NaOH, dioxane; ii, aq. HCl; iii, Dowex 50WX8-200.

attractive new antithrombotic approach that does not rely on the direct inhibition of coagulation. As such, an inhibitor of TAFIa could potentially exhibit antithrombotic efficacy with greatly reduced potential for hemorrhagic side effects compared to an anticoagulant. In this paper we describe the discovery of a series of novel, potent, and selective small molecule inhibitors of TAFIa and the identification of **21** (UK-396,082) as a candidate for clinical evaluation in the treatment of thrombosis and related diseases.[7]

Chemistry

Synthesis of the thiol-containing compounds **4** and **5** (Chart 1) has been reported in the literature.[8] The imidazole-based targets described in this study were prepared as illustrated in Schemes 1−4. Compound **8** was prepared starting from L-histidine methyl ester **22**[9] (Scheme 1). Reductive alkylation of **22** with *tert*-butyl *N*-(2-oxoethyl)carbamate[9] gave the protected intermediate **23**. Hydrolysis of **23** using TFA in methanol/water was followed by saponification and ion exchange chromatography to afford **8**. The (1,4)-substituted alkyl analogues of **8** (compounds **9**−**19**) were prepared (Scheme 2) using a variation of the regiospecific histidine alkylation methodology reported by Jain and Cohen.[10] Thus, intermediate **23** was condensed with carbonyldiimidazole to afford the cyclic intermediate **24**. Alkylation of **24** with the appropriate alkyl bromide or iodide then provided the salt intermediates **25**−**35**, which were subjected to acidic hydrolysis to afford the targets **9**−**19**. Initially, this latter acid hydrolysis step was conducted using

concentrated aqueous hydrochloric acid, in line with the literature precedent. For certain substrates, however, we found that these conditions also led to the generation of an impurity that corresponded to the regioisomeric (1,5)-substituted imidazole. We reasoned that this apparent loss of regiospecificity could stem from a chloride-ion-mediated dealkylation of the salt occurring in competition with the hydrolytic ring-opening reaction. Subsequent ring hydrolysis of this dealkylated intermediate would then provide an unsubstituted imidazole that could react in a non-regioselective manner with the alkyl chloride that had been generated in situ. On the basis of this analysis, the hydrolysis step was examined using concentrated aqueous sulfuric acid in an attempt to avoid such in situ dealkylation (the sulfate counterion being much less nucleophilic than chloride). Notably, under these conditions, the hydrolysis step proceeded without complication to afford the desired analogues as single pure regioisomers.

The racemic targets **6** and **20** were prepared as illustrated in Scheme 3. Deprotonation of triethyl phosphonoacetate **36** with sodium hydride followed by alkylation with the known[11] bromide **37** provided intermediate **38**. Wadsworth−Emmons coupling of **38** with the appropriate imidazole carboxaldehydes **39** or **40** afforded the corresponding alkenes **41** and **42** as mixtures of *E* and *Z* stereoisomers. The imidazolecarboxaldeydes **39** and **40** were readily prepared under standard conditions[12] via alkylation of imidazole 4-carboxaldehyde[9] with 2-(trimethylsilyl)ethoxymethyl chloride (SEMCl) and *n*-propyl bromide, respectively. Reduction of the alkene **41** was achieved by catalytic hydrogenation to afford the protected intermediate **43** as a racemate. In some cases, this catalytic hydrogenation reaction was found to be somewhat capricious because of competitive detritylation and lactam formation. Consequently, a NaBH$_4$/CuCl-mediated conjugate reduction strategy[13] was

Scheme 4[a]
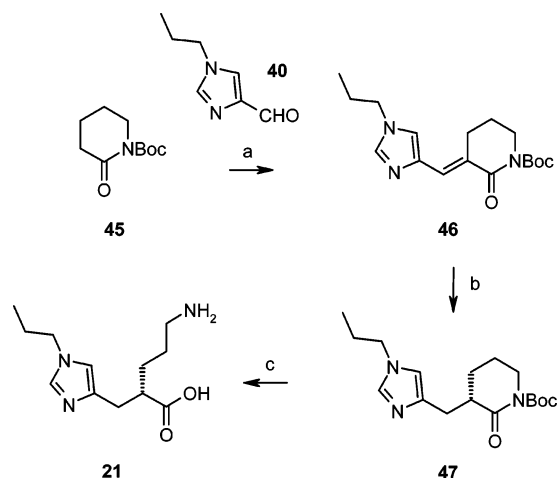
[a] Reagents: (a) i, LHMDS, THF; ii, aldehyde **40**; (b) i, Pd black, H₂, EtOH; ii, chiral HPLC resolution; (c) i, aq. LiOH, THF; ii, aq. HCl; iii, Dowex 50WX8−20.

employed to reduce **42** to the corresponding racemic intermediate **44**. Global deprotection of both **43** and **44** could be achieved via sequential saponification and acid hydrolysis to afford, after ion exchange chromatography, the racemic targets **6** and **20**.

Compound **21** was prepared as a single enantiomer using a lactam-based synthetic strategy (Scheme 4), commencing with the known Boc-substituted piperidinone **45**.[14] Compound **45** was deprotonated with lithium hexamethyldisilazide (LHMDS), and the resultant enolate was treated with carboxaldehyde **40**. Upon workup, the aldol addition product readily dehydrated to afford **46** as a single stereoisomer following chromatography. Catalytic hydrogenation of **46** over palladium-black, and chiral high-performance liquid chromatography (HPLC) resolution of the racemic product provided the intermediate **47** as a single enantiomer (≥99% e.e.). Ring opening of the Boc-substituted lactam moiety in **47** was effected under the mild lithium hydroxide conditions described by Grieco and co-workers,[14] and the product was subjected to acid hydrolysis and ion exchange chromatography to provide **21** (≥95% e.e.). The (2*S*) absolute stereochemistry of **21** (and thus **47**) was evident from an X-ray structural analysis of **21** cocrystallized in porcine pancreatic carboxypeptidase B (pCPB) (*vide infra*). This (2*S*) stereochemistry was subsequently confirmed through single-crystal X-ray crystallography of the heavy-atom containing derivative **49** (Figure 1), which could be readily secured from the known[15] quinidine salt **48** (Scheme 5). An efficient large-scale route to **21** has also recently been reported.[15]

Results and Discussion

At the outset of our program, there had been no reports of potent, nonpeptidic inhibitors of TAFIa.[16,17] However, although carboxypeptidases had attracted little interest as potential drug targets, pioneering historical work on small-molecule inhibitors of pancreatic carboxypeptidases suggested to us that a TAFIa inhibitor could potentially be identified by de novo design. Indeed, the rational design of carboxypeptidase inhibitors in the 1970s proved key landmarks in modern medicinal chemistry and the basis for the discovery of angiotensin-converting enzyme (ACE) inhibitors. For example, in 1973, Byers and Wolfenden[18] demonstrated the "byproduct analogue concept" in the design of benzylsuccinic acid (**1**) as a potent, selective, and competitive inhibitor of bovine pancreatic carboxypeptidase A (CPA). CPA recognizes C-terminal hydrophobic amino acids, and it was
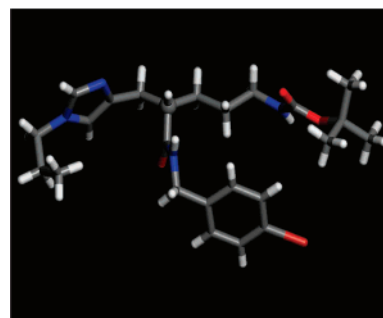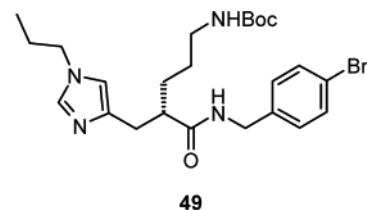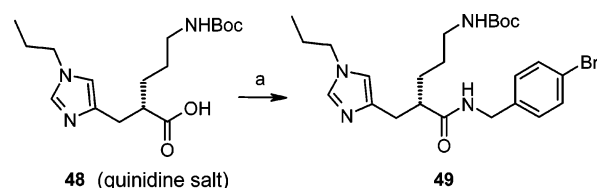

Figure 1. Single-crystal X-ray structure of **49** confirming the (2*S*) stereochemistry of **21**.

Scheme 5[a]

[a] Reagents: (a) EDCI, HOBt, *N*-methyl morpholine, 4-bromobenzylamine, CH₂Cl₂.
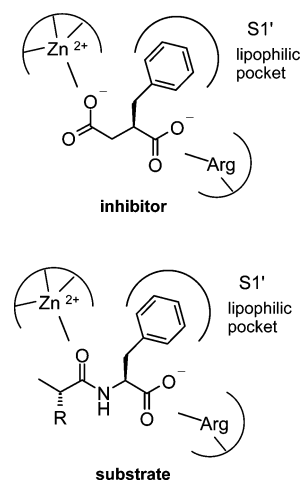

Figure 2. Schematic model of the binding site of CPA illustrating the proposed binding mode of the inhibitor and peptide substrate.

reasoned[19] that **1** binds to CPA as illustrated schematically in Figure 2, with the α-benzyl group in the S1′ specificity pocket, the β-acid moiety binding to the catalytic zinc (mimicking the scissile amide bond in the substrate), and the α-acid mimicking the C-terminal peptide acid. Cushman and Ondetti[20,21] extended the binding model of **1** in CPA to the design of inhibitors for the related zinc-dependent dipeptidase ACE, leading to the discovery of the antihypertensive agent **2** (captopril, (1-[(2*S*)-3-mercapto-2-methylpropionyl]-L-proline) (Chart 1), in which a thiol moiety was utilized as a high affinity ligand for zinc. In addition, Cushman and Ondetti also demonstrated[19] that a thiol moiety could be used as a zinc ligand in carboxypeptidases and illustrated how specificity could be achieved through judicious choice of S1′ substitution. Thus, **3** (SQ-14,603) was found to
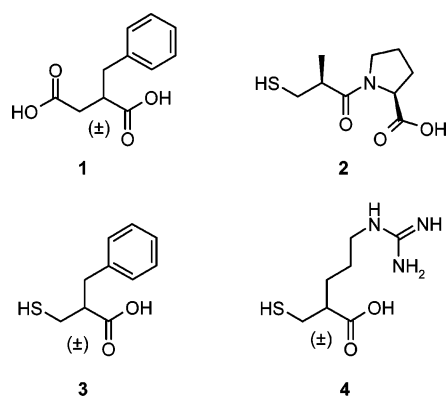
Chart 1

Chart 2

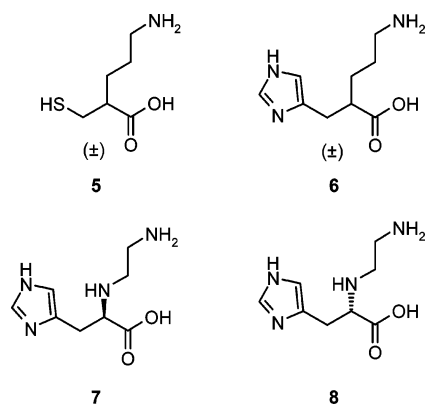**Figure 3.** Schematic model of the binding site of TAFIa illustrating the possible binding modes of compound **8**.

exhibit excellent activity against CPA (Ki = 11 nM) and high selectivity (>10 000-fold) over porcine pancreatic carboxypeptidase B (porcine pCPB), a closely related carboxypeptidase with specificity for C-terminal basic residues (i.e., Arg and Lys). Conversely, replacing the Phe mimetic in **3** with an Arg mimetic gave **4** (SQ-24,798), which exhibited excellent potency for porcine pCPB (Ki = 0.42 nM) and high selectivity over CPA (>10 000-fold). Since porcine pCPB and TAFIa are both basic carboxypeptidases, we decided to prepare **4** and determine its activity against TAFIa. Gratifyingly, **4** proved a highly potent TAFIa inhibitor (Ki = 4 nM) and became the starting point for our SAR program.

Although **4** exhibited excellent activity against TAFIa, further profiling highlighted a number of significant issues with the compound. In particular, attempts to establish the pharmacokinetic properties of **4** were complicated by the instability of the compound in plasma (due to the free thiol group undergoing rapid disulfide conjugation reactions). In addition, we also found **4** to exhibit high potency (Ki = 2 nM) against human plasma carboxypeptidase N (CPN), a result consistent with that obtained previously by Plummer and Ryan.[22] Achieving high selectivity for TAFIa over CPN was a key objective since CPN is known to play a critical role in the clearance of anaphylatoxins such as C5a.[23,24] In light of the inverse selectivity of **4** and the complexity associated the free thiol moiety, attention was turned to the identification of a new template that utilized an alternative to a thiol moiety as the ligand for zinc.

Despite the prevalence of histidine as an endogenous ligand for zinc in proteins, the use of an imidazole moiety as the zinc ligand in metalloprotease inhibitors has been underexplored. Notably, however, Kim and co-workers[25] described a key study on the potential for imidazole to ligate zinc in a series of CPA inhibitors. In light of this work, we decided to investigate whether an imidazole moiety could serve as a replacement for
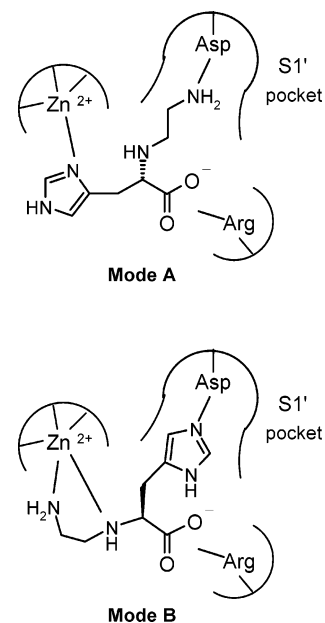
the thiol moiety in **4**. En route to **4**, the simple amino analogue **5** was also prepared[8] and found to exhibit moderate activity against TAFIa (Ki = 300 nM), and compound **6** was therefore identified (Chart 2) as a key target to examine the potential for imidazole-based inhibitors of TAFIa. In addition, while the chemistry to access **6** was in development, compounds **7** and **8** (Chart 2) were identified as analogues of **6** that could be readily assembled from D- or L-histidine, and these compounds were thus prepared for examination as potential TAFIa inhibitors.

Compound **8** proved to be a significant new lead. The compound was a moderately potent, non-thiol inhibitor of TAFIa (Ki = 344 nM) and, in dramatic contrast to the original thiol leads, was inactive against CPN (Ki >10 μM). By comparison, the antipode **7** exhibited only very weak inhibition of TAFIa (Ki = 17 μM). The observation that **8** was significantly more active than **7** at first sight appeared highly surprising: if the imidazole moiety was binding to the catalytic zinc in TAFIa as predicted (Figure 3, Mode A), then the sense of chirality of **8** would be opposite that found in the endogenous peptide substrate. This raised the possibility that **8** could potentially bind to TAFIa in an unexpected orientation in which the imidazole moiety resided in the S1′ specificity pocket and the diamine fragment coordinated zinc (Figure 3, Mode B). Efforts to resolve this binding mode dichotomy through direct cocrystallization and structural elucidation of **8** complexed with TAFIa were unsuccessful. Moreover, attempts to cocrystallize **8** with porcine pCPB as a potential surrogate for TAFIa (*vide infra*) also failed. In the absence of structural information, we embarked on an SAR analysis of **8** with a view towards the optimization of potency against TAFIa.

Potency optimization was sought through the incorporation of hydrophobic binding, and the template was examined for toleration of a methyl substituent probe. In this regard, analysis of imidazole substitution provided promise since the methyl-substituted imidazole analogue **9** exhibited encouraging activity against TAFIa (Table 1). This led us to undertake a full analysis of alkyl-substitution SAR at this position, and data for selected analogues are collected in Table 1. Notably, alkyl chain extension resulted in the optimization of activity against TAFIa, but this reached a plateau between *n*-propyl and *n*-butyl, and further increases in alkyl chain length were detrimental. In

Table 1. TAFIa Inhibition Data for Compounds **8**−**19**
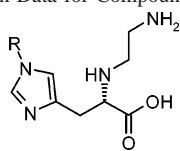
compound	R	Ki (nM)
8	H	344
9	Me	235
10	Et	250
11	*n*-Pr	84
12	*n*-Bu	70
13	*n*-pentyl	160
14	*i*-Pr	430
15	*i*-Bu	100
16	Bn	269
17	phenethyl	140
18	cyclobutylmethyl	124
19	3-hydroxypropyl	111

Chart 3
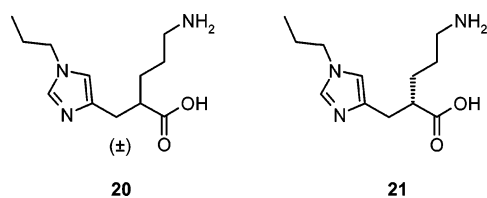
addition, although large lipophilic groups could be well-tolerated (e.g., **17**), groups with larger cone angles (e.g., **16**) were somewhat less favored. These data suggested to us that the *N*-substituent resided in a lipophilic channel that projected out of the active site into solvent. In this context, it was notable that substitution of the alkyl chain with polar functionality was also well-tolerated (e.g., **19**).

The SAR in Table 1 was of particular note in the context of the potential binding modes discussed above (Figure 3). Indeed, if Mode B binding was in operation, such alkyl substitution would serve to localize the imidazole sp^2 lone pair onto the opposite nitrogen to that invoked as having potential to bridge to the specificity Asp at the base of the S1′ pocket. This analysis suggested that the binding mode in which imidazole ligated zinc (Mode A) remained the most likely, despite having the opposite sense of chirality to that of the endogenous peptide. Notably, in this binding mode, the secondary amino functionality in compounds **8**−**19** would potentially be redundant.

On the basis of the above SAR analysis, examination of the original carbon-chain series, exemplified by **6**, continued to represent a key objective. Indeed, a route to this series was secured, and *racemic* **6** (Ki = 140 nM) was found to be a significantly more potent TAFIa inhibitor than (enantiopure) **8**, further supporting the Mode A binding orientation. In addition, the imidazole-substitution SAR established for **8** was found to track directly into this new template, with the racemic *n*-propyl analogue **20** (Chart 3) exhibiting excellent potency against TAFIa (Ki = 46 nM). Resolution confirmed that the binding interaction was also highly stereospecific in this template, and **21** was identified as the preferred enantiomer (Ki = 10 nM, cf. *ent*-**21**, Ki > 700 nM). Enzyme kinetic studies with **21** confirmed the compound as a competitive reversible inhibitor of TAFIa (with a derived Ki of 40 nM by Lineweaver−Burke analysis). Importantly, **21** also exhibited excellent selectivity for TAFIa over CPN (>1000-fold).

Compound **21** was found to exhibit moderate potency against porcine pCPB (Ki = 206 nM), and we decided to attempt the

Table 2. Active Site Sequence Differences within 5.0 Å of the Shell of 21 for Pancreatic Carboxypeptidases[a]

		203	207	243	247	251	254	255
pCPB, *bovine*	*bp*CPB	L...	S...	G...	I...	S...	S	D
pCPB, *porcine*	*pp*CPB	L...	S...	G...	I...	A...	S	D
	TAFIa	V...	S...	G...	L...	P...	G	D

[a] All other residues within 5.0 Å are identical in each species.
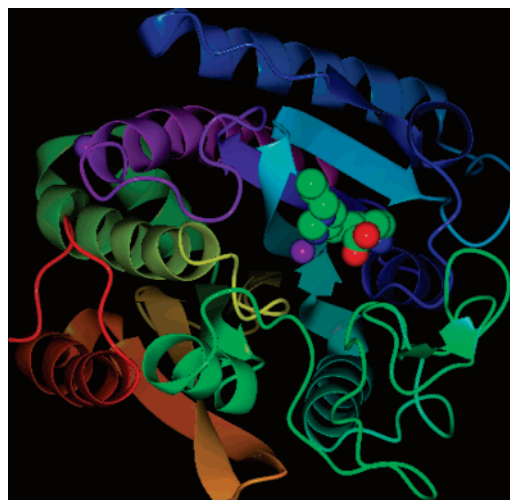
Figure 4. Structure of **21** in porcine pCPB (1.4 Å).
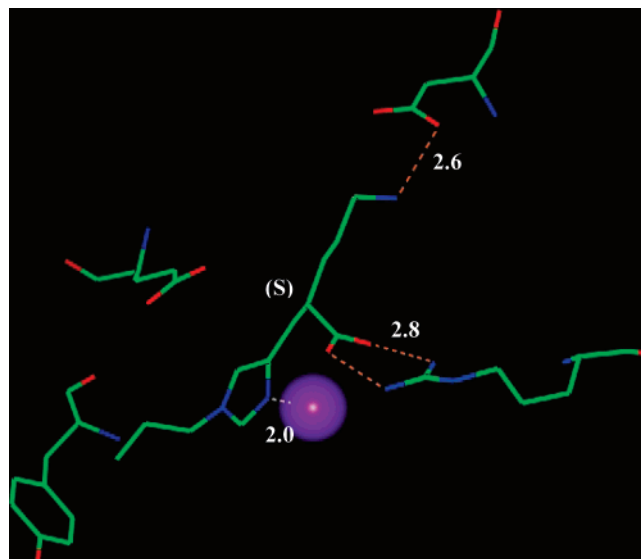
Figure 5. Structure of **21** in porcine pCPB showing key interactions and distances (Å). The catalytic zinc in this representation is displayed as a purple sphere.

cocrystallization of **21** with porcine pCPB as a surrogate for TAFIa. Porcine pCPB was considered a suitable TAFIa surrogate due to its high degree of sequence identity (80%) in the active site region (Table 2). Additionally, homology models of TAFIa based on the available carboxypeptidase structures predicted that none of the residues that differed between porcine pCPB and TAFIa would be significantly involved in inhibitor binding. Attempts to cocrystallize **21** with porcine pCPB were successful, and the X-ray structure of the complex was determined to high resolution (1.4 Å) (Figure 4). Examination of the active site of this structure (Figure 5) confirmed our SAR analysis that the imidazole moiety in **21** was indeed involved in ligation of the catalytic zinc (Mode A). *This crystallographic data further highlights the utility of an imidazole moiety as a suitable zinc ligand in zinc-metalloprotease inhibitors.* The

remaining key interactions were also as predicted (Figure 5):[26] the primary amine in **21** bridged to the key Asp255 at the base of the S1′ specificity pocket, the acid moiety formed a salt bridge with Arg145, mimicking the C-terminal acid of the substrate, and the imidazole alkyl substituent was found to reside in a lipophilic channel, which projected out of the active site into solvent, adjacent to Tyr 199. Finally, this high-resolution structure indicated that the absolute configuration of **21** was (2*S*) (Figure 5), in line with the stereochemistry of **8**. The observation that **21** has an opposite stereochemical orientation relative to the endogenous peptide substrate is very interesting and may reflect the geometric constraints associated with a highly directional imidazole–zinc interaction. Further, the ability of TAFIa to accommodate a ligand with this stereochemistry may also provide a rationale for the high CPN selectivity of **21** relative to the original thiol-based lead **4**.

The antithrombotic potential of TAFIa inhibition was established through exploring the efficacy of **21** in rabbit models of venous thrombosis and surgical bleeding. Compound **21** demonstrated efficacy in the thrombosis model with a maximal inhibition of thrombus formation of approximately 35%, yet caused *no increase in bleeding* in the surgical blood loss model when compared to vehicle-treated animals. In contrast, administration of *t*-PA caused a 66% inhibition in thrombus generation, but this was associated with a dramatic (14-fold) increase in blood loss. These data support the conclusion that TAFIa inhibitors have potential as novel, stand-alone antithrombotic agents with significantly enhanced safety margins over established agents.[27]

The pharmacokinetics of **21** were found to be fully consistent with its physicochemical properties of low molecular weight (MW = 239) and high hydrophilicity (log *D* = −2.8). Following intravenous (iv) bolus administration in a dog (0.6 mg/kg), **21** had pharmacokinetics characterized by low total plasma clearance (Clp = 3.1 mL/min/Kg), commensurate with passive renal elimination (glomerular filtration rate (GFR) in dogs ≈ 3 mL/min/Kg), and a very low volume of distribution (0.35 L/Kg). Renal elimination was confirmed by urinary excretion studies in a dog in which 96% of an iv dose of **21** was recovered in the urine as unchanged drug. The terminal elimination half-life of **21** in a dog was 1.4 h and, on the basis of oral dog pharmacokinetic studies (1 mg/kg), oral bioavailability was found to be 42%. Since **21** displayed exclusively non-hepatic clearance in the dog, this moderate bioavailability likely reflects incomplete absorption of **21** via the *paracellular* route. Indeed, **21** was found to have negligible flux across Caco-2 monolayers, confirming that transcellular absorption was unlikely.[28] Since a rat is considered a more reliable predictor of paracellular absorption potential in man,[29] the absorption of **21** in this species was also assessed. Gratifyingly, **21** was found to exhibit ∼20% absorption in the rat, suggesting that the compound had excellent potential for bioavailability in humans. On the basis of the above studies, compound **21** was selected for clinical development.

In Phase I clinical studies, compound **21** was very well-tolerated and exhibited an excellent pharmacokinetic profile, fully consistent with the preclinical predictions. Human half-life following iv dosing was found to be 4 h, characterized by a low total clearance (Clp = 1.5−2 mL/min/Kg), in line with human GFR, and a low volume of distribution (0.5 L/Kg). Oral-dosing of **21** confirmed good oral bioavailability (F_{oral} = 23%), a T_{max} of 4−6 h, and dose-linear pharmacokinetics. Notably, bioavailability and T_{max} were not effected by co-administration of **21** with food.

Conclusion

In this paper, we have described a novel series of inhibitors of TAFIa that utilize imidazole as a zinc ligand. These studies led to the identification of **21** as a potent (Ki = 10 nM), highly selective (sel. TAFIa/CPN > 1000) competitive inhibitor of TAFIa. Compound **21** exhibited antithrombotic efficacy in a rabbit model of venous thrombosis, yet had no effect on surgical bleeding in the rabbit. In addition, **21** exhibited excellent preclinical and clinical pharmacokinetics characterized by good paracellular absorption, low clearance, and a low volume of distribution, fully consistent with its physicochemical properties of low molecular weight (MW = 239) and high hydrophilicity (log *D* = −2.8). These data indicate **21** has potential as a novel TAFIa inhibitor for the treatment of thrombosis and related fibrin-dependent diseases in humans.

Experimental Section

(A) Biology. (1) Assay for Inhibition of TAFIa. (i) TAFI Activation. Human TAFI (recombinant or purified) was activated by incubating 20 μL of stock solution (360 μg/mL) with 10 μL of human thrombin (10 NIH units/mL), 10 μL of rabbit thrombomodulin (30 μg/mL), 6 μL of calcium chloride (50 mM) in 50 μL of 20 mM *N*-[2-hydroxyethyl]piperazine-*N*-[2-ethanesulfonic acid] (HEPES) buffer containing 150 mM sodium chloride and 0.01% TWEEN 80 (polyoxyethylene–sorbitan monooleate), pH 7.6, for 20 min at 22 °C. At the end of the incubation period, thrombin was neutralized by the addition of 10 μL of PPACK (D-Phe-Pro-Arg chloromethyl ketone) (100 nM). TAFIa solution was stored on ice for 5 min and finally diluted with 175 μL of HEPES buffer.

(ii) Ki Determination (TAFIa). A number of different dilutions of the test compound in water were made up. To 20 μL of each dilution was added 150 μL of HEPES buffer and 10 μL of TAFIa, which was then preincubated for 15 min at 24 °C. To each dilution was then added 20 μL furylacryloyl-alanyl-lysine at a standard concentration. Substrate turn over was measured by reading the absorbance of the reaction mixture at 330 nm every 15 s for 30 min. The reaction was performed at 24 °C, and samples were mixed for 3 s prior to each absorbance reading. A graph of percent inhibition against test compound concentration was then plotted, from which the IC_{50} value was calculated. The Ki value was then calculated using the Cheng–Prusoff equation.

(iii) Effects of Compound 21 in Rabbit Models of Venous Thrombosis and Surgical Bleeding. Thrombus formation in the anesthetized rabbit (New Zealand White, Harlan, male, 2.0−3.0 kg) was induced by the insertion of a collagen-coated thread into both jugular veins for 1 h, after which the thrombi were removed and weighed. Intravenously administered **21** had no effect on thrombus weight at projected free plasma concentrations of below 80 nM (*n* = 3; estimated to be approximately 8 nM), but at approximately 80 nM (*n* = 6) it caused a significant 37% inhibition in thrombus weight compared to that in vehicle-treated animals (*n* = 10). Increasing the free plasma concentrations of **21** had no greater inhibitory effect. In comparison, *t*-PA (10 μg/kg/min; *n* = 6), at a dose that caused a significant 45% depletion in circulating fibrinogen, caused a significant 66% inhibition in thrombus generation compared to that in vehicle-treated animals (*n* = 13). To confirm the antithrombotic activity and maximal effect of **21**, a repeat study was carried out. **21** (at approximately 800 nM; *n* = 6) caused a significant 36% inhibition of thrombus formation compared to vehicle-treated animals (*n* = 5). In an additional group of anesthetized rabbits, **21**, at a dose (100 μg/kg/min pretreated for 30 min and infused throughout; *n* = 3) that is estimated to have achieved a free plasma concentration of approximately 80 μM, had no effect on surgical blood loss when compared to that of vehicle-treated animals (*n* = 4). In contrast, t-PA, infused at a dose (10 μg/kg/min; *n* = 4) that caused a 66% inhibition in thrombus generation in the efficacy study, caused an approximately 14-fold increase in surgical bleeding (mean increase from 1 to 14 g total blood loss). All the above in vivo studies involved terminal

anaesthesia of the rabbits, were conducted in compliance with national legislation, and were ethically reviewed.

(B) Chemistry. Melting points were determined on a Gallenkamp melting point apparatus using glass capillary tubes and were uncorrected. Unless otherwise indicated, all reactions were carried out under a nitrogen atmosphere, using commercially available anhydrous solvents. The term"0.88 Ammonia" refers to a commercially available aqueous ammonia solution of about 0.88 specific gravity. Thin-layer chromatography was performed on glass-backed precoated Merck silica gel (60 F254) plates, and compounds were visualized using UV light, 5% aqueous potassium permanganate, or chloroplatinic acid/potassium iodide solution. Silica gel column chromatography was carried out using 40−63 μm silica gel (Merck silica gel 60). Ion exchange chromatography was performed using DOWEX 50WX8-200 ion-exchange resin that had been prewashed with deionized water. Proton NMR spectra were measured on a Varian Inova 300, Varian Inova 400, or Varian Mercury 400 spectrometer in the solvents specified. In the NMR spectra, only exchangeable protons that appeared distinct from the solvent peaks are reported. Low-resolution mass spectra (LRMS) were recorded on either a Fisons Trio 1000, using thermospray positive ionization, or a Finnigan Navigator, using electrospray positive or negative ionization. High-resolution mass spectra (HRMS) were recorded on a Bruker Apex II FT-MS using electrospray positive ionization. Combustion analyses were conducted by Exeter Analytical U.K. Ltd., Uxbridge, Middlesex, U.K. Optical rotations were determined at 25 °C using a Perkin-Elmer 341 polarimeter using the solvents and concentrations specified.

(1) (2S)-2-[(2-Aminoethyl)amino]-3-(1H-imidazol-4-yl)propanoic Acid (8). Trifluoroacetic acid (17 mL) was added dropwise to a stirred solution of **23** (2.58 g, 8.2 mmol) in methanol/water (27:14 mL). The reaction was slightly exothermic with evolution of carbon dioxide gas. The mixture was stirred at room temperature for 4 h, and the solvent was removed by evaporation under reduced pressure to give a colorless oil, which was dried in vacuo overnight. The resultant oil was treated with aqueous sodium hydroxide solution (1 N) until the solution was at pH = 8. A further portion of aqueous sodium hydroxide solution (1 N, 30 mL) was added, and the solution was stirred at room temperature for 72 h. The solution was concentrated under reduced pressure to 10 mL and purified by ion exchange chromatography (DOWEX 50WX8-200), eluting with a solvent gradient of deionized water/0.88 ammonia solution (100:0 to 97:3). The solvent was removed by evaporation under reduced pressure to afford a yellow oil, which was dissolved in deionized water (15 mL) and freeze-dried overnight to afford a foam. This material was dissolved in deionized water/methanol (95:5) and further purified using MCI gel (55 g) chromatography, eluting with a solvent gradient of deionized water/methanol (95:5) to afford the title compound, 1.13 g, 69% yield. ^{1}H NMR (D$_2$O, 300 MHz) δ: 2.61−2.87 (m, 4H), 2.92 (m, 2H), 3.25 (t, 1H), 6.81 (s, 1H), 7.59 (s, 1H). LRMS: m/z 199.2 (MH$^+$). [α]$_D$ = +1.74 (c 0.12, deionized water). Anal. (C$_8$H$_{14}$N$_4$O$_2$·1.3H$_2$O) C, H, N.

(2) General Procedure for Hydrolysis of Salts 25−35 (Method B). Either concentrated hydrochloric acid (6 N, 5 mL) or concentrated sulfuric acid (2−4 N, 5 mL) was added to a stirred solution of the requisite salt **25−35** (0.32 mmol) in water (5 mL), and the mixture was heated at reflux for 17 h. The mixture was allowed to cool to room temperature, and the solvent was removed by evaporation under reduced pressure. The residue was purified by ion exchange chromatography (DOWEX 50WX8-200), eluting with deionized water/0.88 ammonia (97:3).

(3) (2S)-2-[(2-Aminoethyl)amino]-3-(1-methyl-1H-imidazol-4-yl)propanoic Acid (9). Prepared from the product of **25** according to Method B (using concd H$_2$SO$_4$) and isolated in 52% yield: ^{1}H NMR (D$_2$O, 400 MHz) δ: 2.60−2.80 (m, 4H), 2.90 (m, 2H), 3.24 (t, 1H), 3.53 (s, 3H), 6.77 (s, 1H), 7.45 (s, 1H). LRMS: m/z 211 (M$^+$). [α]$_D$ = −5.8 (c 0.12, methanol). Anal. (C$_9$H$_{16}$N$_4$O$_2$·1.45H$_2$O) C, H, N.

(4) (2S)-5-Amino-2-[(1-n-propyl-1H-imidazol-4-yl)methyl]pentanoic Acid (21). Lithium hydroxide monohydrate (1.1 g, 28

mmol) and water (28 mL) were added to a solution of the lactam **47** (3 g, 9.33 mmol) in tetrahydrofuran (THF; 45 mL), and the reaction was stirred at room temperature for 18 h. The solution was neutralized using aqueous hydrochloric acid (6 N), then more acid (15 mL, 6 N) was added, and the solution was stirred at room temperature for 4 h. The mixture was purified directly by ion exchange chromatography (DOWEX 50WX8-200), eluting with a solvent gradient of deionized water/0.88 ammonia (100:0 to 97:3), to give the title compound as a white solid, 2.1 g, 94% yield. ^{1}H NMR (D$_2$O, 400 MHz) δ: 0.60 (t, 3H), 1.30 (m, 2H), 1.40 (m, 2H), 1.55 (m, 2H), 2.26−2.40 (m, 2H), 2.57 (dd, 1H), 2.76 (m, 2H), 3.68 (t, 2H), 6.66 (s, 1H), 7.36 (s, 1H). HRMS: m/z 240.1699 (MH$^+$), calcd 240.1706. [α]$_D$ = +2.80 (c 0.14, deionized water). [α]$_D$ = −4.9 (c 0.16, methanol). [α]$_D$ = −5.0 (c 0.10, ethanol), ≥95% e.e. by capillary electrophoresis analysis. Anal. (C$_{12}$H$_{21}$N$_3$O$_2$· 0.3H$_2$O) C, H, N.

(5) Methyl (2S)-2-({2-[(tert-Butoxycarbonyl)amino]ethyl}-amino)-3-(1H-imidazol-4-yl)propanoate (23). l-Histidine methyl ester **22** (7.93 g, 32.8 mmol) and sodium acetate (10.75 g, 131 mmol) were added to a stirred solution of *tert*-butyl N-(2-oxoethyl)-carbamate (5.22 g, 32.8 mmol) in methanol (100 mL). Molecular sieves (4 Å) and sodium cyanoborohydride (4.12 g, 65.6 mmol) were added, and the mixture was stirred at room temperature for 17 h. Aqueous hydrochloric acid (2N, 4 mL) was added, and the mixture was then basified with saturated aqueous sodium carbonate solution to pH = 10. The mixture was filtered to remove solid, which was washed with methanol. Methanol was removed by evaporation under reduced pressure, and the residual aqueous solution was extracted with ethyl acetate (2 × 300 mL). The combined organic extracts were then dried (MgSO$_4$), filtered, and concentrated under reduced pressure. The resultant residue was purified by column chromatography on silica gel, eluting with a solvent gradient of dichloromethane/methanol (96:4 to 92:8), to afford the title compound as a colorless oil, 8.07 g, 79% yield. ^{1}H NMR (CDCl$_3$, 300 MHz) δ: 1.42 (s, 9H), 2.65 (m, 1H), 2.90 (m, 2H), 3.07 (m, 1H), 3.19 (m, 1H), 3.30 (m, 1H), 3.58 (m, 1H), 3.73 (s, 3H), 5.22 (br s, 1H), 6.97 (s, 1H), 7.02 (br s, 2H), 7.91 (s, 1H). LRMS: m/z 313.1 (MH$^+$).

(6) Methyl (7S)-6-{2-[(tert-Butoxycarbonyl)amino]ethyl}-5-oxo-5,6,7,8-tetrahydroimidazo[1,5-c]pyrimidine-7-carboxylate (24). Carbonyldiimidazole (156 mg, 0.959 mmol) was added to a stirred solution of **23** (300 mg, 0.959 mmol) in N,N-dimethylformamide (5 mL), and the mixture was heated at 60−70 °C for 17 h. The solvent was removed by evaporation under reduced pressure, and the residue was dissolved in saturated aqueous sodium hydrogen carbonate solution and extracted with dichloromethane. The combined organic extracts were dried (MgSO$_4$), filtered, and then concentrated under reduced pressure. The residue was purified by column chromatography on silica gel, eluting with dichloromethane/methanol (95:5), to afford the title compound as a colorless oil, 210 mg, 67% yield. ^{1}H NMR (D$_2$O, 300 MHz) δ: 1.40 (s, 9H), 3.20−3.60 (m, 5H), 3.70 (s, 3H), 4.08 (m, 1H), 4.33 (m, 1H), 4.82 (br m, 1H), 6.80 (s, 1H), 8.13 (s, 1H). LRMS: m/z 339 (MH$^+$). [α]$_D$ = +39.2 (c 0.12, dichloromethane).

(7) General Procedure for Alkylation of 24 (Method A). The appropriate alkyl bromide or iodide (2−5 equiv) was added to a stirred solution of **24** (200 mg, 0.592 mmol) in acetonitrile (5 mL), and the mixture was heated at reflux for 17 h under a nitrogen atmosphere. The mixture was allowed to cool to room temperature, and the solvent was removed by evaporation under reduced pressure. The residue was purified by column chromatography on silica gel, eluting with dichloromethane/methanol (90:10), to afford the product salts **25−35**.

(8) (7S)-6-{2-[(tert-Butoxycarbonyl)amino]ethyl}-7-(methoxy-carbonyl)-2-methyl-5-oxo-5,6,7,8-tetrahydroimidazo[1,5-c]pyrimidin-2-ium Iodide (25). Prepared according to Method A using methyl iodide (3 equiv) and isolated in 75% yield. ^{1}H NMR (DMSO, 400 MHz) δ: 1.32 (s, 9H), 3.09−3.23 (m, 3H), 3.45 (m, 2H), 3.64 (s, 3H), 3.86 (s, 3H), 3.95 (m, 1H), 4.86 (m, 1H), 6.91 (s, 1H), 7.60 (s, 1H), 9.80 (s, 1H). [α]$_D$ = +36.2 (c 0.11, methanol). Anal. (C$_{16}$H$_{15}$N$_4$O$_5$I·1.25H$_2$O) C, H, N.

(9) ***tert*-Butyl (3*E*)-2-Oxo-3-[(1-*n*-propyl-1*H*-imidazol-4-yl)-methylene]-1-piperidinecarboxylate (46).** A solution of lithium bis(trimethylsilyl)amide in THF (43.5 mL, 1 M, 43.5 mmol) was added dropwise to a cooled (−78 °C) solution of *tert*-butyl 2-oxo-1-piperidinecarboxylate **45**[13] (8.7 g, 43.5 mmol) in THF (120 mL), and, once the addition was complete, the solution was allowed to warm to 0 °C and then stir for an hour. The solution was recooled to −78 °C, a solution of the aldehyde **40** (4 g, 28.9 mmol) in THF (40 mL) was added, and the reaction was then allowed to warm to room temperature. The reaction mixture was stirred for 18 h and then partitioned between water and ethyl acetate. The phases were separated, and the organic phase was dried (MgSO$_4$), filtered, and concentrated under reduced pressure. The residue was purified by column chromatography on silica gel, eluting with dichloromethane/methanol (95:5), to give the title compound, 4 g, 43% yield. ^{1}H NMR (CDCl$_3$, 300 MHz) δ: 0.89 (t, 3H), 1.50 (s, 9H), 1.78 (m, 2H), 1.86 (m, 2H), 3.00 (m, 2H), 3.70 (t, 2H), 3.85 (t, 2H), 7.07 (s, 1H), 7.46 (s, 1H), 7.62 (s, 1H). LRMS: *m/z* 320.3 (MH$^+$).

(10) ***tert*-Butyl (3*S*)-2-Oxo-3-[(1-propyl-1*H*-imidazol-4-yl)-methyl]-1-piperidinecarboxylate (47).** A mixture of **46** (6.6 g, 20.6 mmol) and palladium black (700 mg) in ethanol (120 mL) was hydrogenated at 4 atm and 60 °C for 18 h. The cooled mixture was filtered through Arbocel, washing through with ethyl acetate, and the filtrate concentrated under reduced pressure. The crude product was purified by column chromatography on silica gel, eluting with dichloromethane/methanol (97:3), to afford the race-mate of the title compounds as a yellow oil, 4.3 g, 65% yield. This racemic compound was resolved by HPLC using a Chiralcel OG 250 column (20 mm) and hexane/isopropanol (70:30) as eluant, at a rate of 10 mL/minute, to give the title compound (1.56 g, retention time 15.23 min, 98.9% e.e.) and its antipode (1.56 g, retention time 10.10 min, 99.5% e.e.). Data for **47**: ^{1}H NMR (CDCl$_3$, 300 MHz) δ: 0.92 (t, 3H), 1.54 (s, 9H), 1.80 (m, 4H), 2.00 (m, 2H), 2.63−2.85 (m, 2H), 3.19 (m, 1H), 3.58 (m, 1H), 3.90−3.98 (m, 3H), 6.72 (s, 1H), 7.37 (s, 1H). LRMS: *m/z* 322.3 (MH$^+$). [α]$_D$ = +27.7 (*c* 0.22, dichloromethane).

(11) **(2*S*-*N*-(4-Bromobenzyl)-5-[(*tert*-butoxycarbonyl)amino]-2-[(1-*n*-propyl-1H-imidazol-4-yl)methyl]pentanamide (49).** 1-(3-Dimethylaminopropyl)-3-ethylcarbodiimide hydrochloride (EDCI) (2.9 g, 1.5mmol) was added to a stirred mixture of known quinidine salt **48**[15] (1 g, 1.5 mmol), 1-hydroxybenzotriazole hydrate (HOBt) (0.205 g, 1.5 mmol), *N*-methyl morpholine (0.33 mL, 3 mmol) and 4-bromo benzylamine (2.8 g, 1.5 mmol) in dry CH$_2$Cl$_2$ at 0−5 °C. The mixture was allowed to warm to room temperature and was stirred for 72 h. The resultant solution was then concentrated under reduced pressure, and the residue was suspended in saturated sodium carbonate solution (20 mL) and then extracted with ethyl acetate (3 × 20 mL). The ethyl acetate solution was then dried (Na$_2$SO$_4$), filtered, and concentrated under reduced pressure. The crude product was purified by column chromatography on silica gel, using an elution gradient of dichloromethane/methanol (100:0 to 97.5:2.5), to give the title compound as a glass following suspension and evaporation from ether, 0.6 g, 80% yield. The glass was recrystal-lized from ethyl acetate/hexane to give colorless crystals, which were filtered and dried and confirmed to be ≥99.5% e.e. by chiral HPLC (chiral column OG250 × 4.6 mm; retention time 5.92). ^{1}H NMR (CDCl3, 400 MHz) δ: 0.90 (t, 3H), 1.43 (s, 9H), 1.49−1.53 (m, 3H), 1.69−1.78 (m, 3H), 2.66−2.85 (m, 2H), 3.76 (t, 2H), 4.17 (dd, 1H), 4.40 (dd, 1H), 4.65 (s, 1H), 6.58 (s, 1H), 6.73 (s, 1H), 7.00 (d, 2H), 7.28 (s, 1H), 7.37 (d, 2H). LRMS: *m/z* 506.5, 508.5 (MH$^+$). [α]$_D$ = −10.7 (*c* 0.103, methanol). MPt 102−103 °C. Anal. (C$_{24}$H$_{35}$BrN$_4$O$_3$) C, H, N. Recrystallization of a small (50 mg) sample of the crystalline product from ethyl acetate/hexane gave single crystals of **49** suitable for X-ray crystallography studies (confirming absolute configuration as *S*).

(C) Crystallization, X-ray Data Collection and Structure Solution for Compound 21 in Porcine pCPB (Figure 4). Porcine pCPB was purchased from Sigma (C6158) in the activated form. The protein was dissolved in Milli-Q water at a concentration of 10 mg/mL. Inhibitor complex was preformed with a 60-fold molar excess of inhibitor dissolved in Milli-Q water. Crystals of the complex with **21** were grown by vapor diffusion (2 μL protein and 2 μL reservoir buffer) using the hanging drop method. The reservoir was 100 mM NaKPO$_4$, pH 6.8; 200 mM zinc acetate; 10% PEG8000. Precipitate, which formed upon mixing of the reservoir solution, was removed by centrifugation. Crystals grew over a period of several weeks and were of tetragonal form, space group *P*4$_1$2$_1$2, with cell dimensions *a* = 82.248, *b* = 82.248, and *c* = 93.761 Å and α = β = γ = 90.0. Crystals were cryoprotected using 25% glycerol, and data were collected to 2.0 Å at 100 °K on a Rigaku RU-H3R and R-axis IV image plate. Additional data, on the same sample, was collected to 1.4 Å at the ESRF on station ID14 EH2. All data were processed using DENZO.[30] The data were combined for refinement with an overall *R* merge of 9% for all data and completeness of 98.5% in the final resolution shell between 1.45 and 1.4 Å.

All data reduction and subsequent refinement were performed using the CCP4 program suite.[31] The structure was solved by molecular replacement methods using the program AMORE.[32] The deposited coordinates pdb1nsa.ent were used to build a search model where the pro-domain residues were removed. Analysis clearly identified the presence of the inhibitor **21** in the active site of the protein. Additionally the high-resolution structure indicated se-quence anomalies with the deposited sequence in the PDB entry 1NSA. A patent publication US 5672496-A reveals a corrected sequence (PID gi2731308) for porcine pancreatic carboxypeptidase B, with which this high-resolution structure is in agreement (as used in more recent PDB structural deposition 1Z5R). Sequence changes and modeling of the inhibitor were performed using the graphics program QUANTA.

The structure was refined using REFMAC[31] with the inclusion of two zinc atoms and 305 solvents molecules with a final *R* factor of 19% and an *R*$_{free}$[33] of 21%. The Ramachandran conformational parameters generated by PROCHECK[34] indicate that the structure is in accordance with expected values.

Coordinates for this complex have been deposited with the Protein Data Bank (PDB code2JEW).

(D) X-ray Data Collection and Structure Solution for Compound 49 (Figure 1). X-ray diffraction data were recorded at room temperature using a Bruker AXS SMART-APEX CCD area-detector diffractometer (Mo Kα radiation). Intensities were inte-grated[35] from several series of exposures. Each exposure covered 0.3° in ω, with an exposure time of 60 s, and the total data set was more than a sphere. Data were corrected for absorption using the multiscans method.[36] The crystal structure was solved by direct methods using SHELXS-97[37] and refined by the method of least-squares using SHELXL-97.[38]

There were two molecules in the asymmetric unit, each with the same chirality (ORTEP drawings of both molecules are included in Supporting Information, Figure 6). Refinement of the structure proceeded normally, although the propyl groups of both molecules were found to be disordered, and each were modeled over two overlapping conformations. The occupancy of the two conforma-tions was determined from a refinement job where the thermal parameters of the atoms in question were fixed at some reasonable value while their occupancies were allowed to refine; atoms in the same group were assigned a common occupancy, while occupancies of the two conformations were constrained to sum to 1. In this way, the two propyl orientations in both molecules were found to have a 0.5 occupancy. The occupancies were fixed at these values for all subsequent jobs. Mild restraints were placed on these disordered groups to give them a reasonable geometry.

All heavy atoms were refined with anisotropic temperature factors, except those in the disordered propyl groups which were refined with isotropic temperature factors. All hydrogen atoms were placed in calculated positions and allowed to refine with a riding model and isotropic temperature factors.

Pertinent crystal, data collection, and structure refinement details are summarized in the Supporting Information (Table 3). Atomic coordinates, bond lengths, bond angles, torsion angles, and tem-perature factors are also included in the Supporting Information (Tables 4−8).

The absolute configuration for this structure was determined by the method of Flack.[39] Both molecules in the asymmetric unit were found to have an 'S' configuration at the chiral center, for a final refined Flack parameter of −0.016 (7).

Supporting Information Available: ORTEP plots and crystal structure data for compound **49**. Experimental details for compounds **6**, **10**−**20**, **26**−**35**, and **38**−**44**. Analytical data for target compounds **6** and **8**−**21** and selected intermediates. This material is available free of charge via the Internet at http://pubs.acs.org.

References

(1) Bajzar, L.; Manuel, R.; Nesheim, M. E. Purification and characterization of TAFI, a thrombin-activatable fibrinolysis inhibitor. *J. Biol. Chem.* **1995**, *270*, 14477−14484.

(2) (a) Nesheim, M. E. TAFI. *Fibrinolysis Proteolysis* **1999**, *13*, 72−77. (b) Nesheim, M.; Wang, W.; Boffa, M.; Nagashima, M.; Morser, J.; Bajzar, L. Thrombin, thrombomodulin and TAFI in the molecular link between coagulation and fibrinolysis. *Thromb. Haemostasis* **1997**, *78*, 386−391.

(3) For recent reviews on TAFI, see: (a) Willemse, J. L.; Hendriks, D. F. A role for procarboxypeptidase U (TAFI) in thrombosis. *Front. Biosci.* **2007**, *12*, 1973−1987. (b) Mosnier, L. O.; Bouma, B. N. Regulation of fibrinolysis by thrombin activatable fibrinolysis inhibitor, an unstable carboxypeptidase B that unites the pathways of coagulation and fibrinolysis. *Arterioscler., Thromb., Vasc. Biol.* **2006**, *26*, 2445−2453. (b) Marx, P. F. Thrombin-activatable fibrinolysis inhibitor. *Curr. Med. Chem.* **2004**, *11*, 2335−2348.

(4) Eaton, D. L.; Malloy, B. E.; Tsai, S. P.; Henzel, W.; Dryana, D. Isolation, molecular cloning, and partial characterisation of a novel carboxypeptidase B from human plasma. *J. Biol. Chem.* **1991**, *266*, 21833−21838.

(5) Wang, W.; Hendriks, D. F.; Scharpe S. S. Carboxypeptidase U, a plasma carboxypeptidase with high affinity for plasminogen. *J. Biol. Chem.* **1994**, *269*, 15937−15944.

(6) Refino, C. J.; DeGuzman, L.; Schmitt, D.; Smyth, R.; Jeet, S.; Lipari, M. T.; Eaton, D.; Bunting, S. Consequences of inhibition of plasma carboxypeptidase B on *in vivo* thrombolysis, thrombosis, and hemostasis. *Fibrinolysis Proteolysis* **2000**, *14*, 305−314.

(7) Allerton, C. M. N.; Blagg, J.; Bunnage, M. E. Steele, J. PCT Int. Appl. WO 2002014285, 2002.

(8) Ondetti, M. A.; Condon, M. E. U.S. Patent 4146611, 1979.

(9) Commercially available from Aldrich Chemical Company.

(10) Jain, R.; Cohen, L. A. Regiospecific alkylation of histidine and histamine at N-1 (τ). *Tetrahedron* **1996**, *52*, 5363−5370.

(11) Huszthy, P.; Bradshaw, J. S.; Krakowiak, K. E.; Wang, T.; Dalley, N. K. Efficient synthesis of azetidine through *N*-trityl- or *N*-dimethoxytritylazetidines starting from 3-amino-1-propanol or 3-halopropylamine hydrohalides. *J. Heterocycl. Chem.* **1993**, *30*, 1197−1207.

(12) Aldabbagh, F.; Bowman, W. R.; Mann, E.; Slawin, A. M. Z. Bu₃SnH mediated oxidative radical cyclisation onto imidazoles and pyrrole. *Tetrahedron* **1999**, *55*, 8111−8128.

(13) Narisada, M.; Horibe, I.; Watanabe, F.; Takeda, K. Selective reduction of aryl halides and a,b-unsaturated esters with sodium borohydride-cuprous chloride in methanol and its application to deuterium labeling. *J. Org. Chem.* **1989**, *54*, 5308−5313.

(14) Flynn, D. L.; Zelle, R. E.; Grieco, P. A. A mild two-step method for the hydrolysis/methanolysis of secondary amides and lactams. *J. Org. Chem.* **1983**, *48*, 2424−2426.

(15) Appleby, I; Boulton, L. T.; Cobley, C. J.; Hill, C.; Hughes, M.; De Koning, P. D.; Lennon, I. C.; Praquin, C.; Ramsden, J. A.; Samuel, H. J.; Willis, N. Efficient synthesis of an imidazole-substituted d-amino acid by the integration of chiral technologies. *Org. Lett.* **2005**, *7*, 1931−1934.

(16) The potato tuber carboxypeptidase inhibitor peptide (PCI) had been shown to be a potent inhibitor of TAFIa: Bajzar, L.; Nesheim, M. E.; Tracy, P. B. The profibrinolytic effect of activated protein C in clots formed from plasma is TAFI-dependent. *Blood* **1996**, *88*, 2093−2100.

(17) Over recent years, a number of nonpeptidic TAFIa inhibitors have been disclosed, including a related series of imidazole-based inhibitors from Merck; see: (a) Barrow, J. C.; Nantermet, P. G.; Stauffer, S. R.; Ngo, P. L.; Steinbeiser, M. A.; Mao, S.-S.; Carroll, S. S.; Bailey, C.; Colussi, D.; Bosserman, M.; Burlein, C.; Cook, J. J.; Sitko, G.; Tiller, P. R.; Miller-Stein, C. M.; Rose, M.; McMasters, D. R.; Vacca, J. P.; Selnick, H. G. Synthesis and evaluation of imidazole acetic acid inhibitors of activated thrombin-activatable fibrinolysis inhibitor as novel antithrombotics. *J. Med. Chem.* **2003**, *46*, 5294−5297. (b) Nantermet, P. G.; Barrow, J. C.; Lindsley, S. R.; Young, M.; Mao, S.-S.; Carroll, S.; Bailey, C.; Bosserman, M.; Colussi, D.; McMasters, D. R.; Vacca, J. P.; Selnick, H. G. Imidazole acetic acid TAFIa inhibitors: SAR studies centered around the basic P1′ group, *Bioorg. Med. Chem. Lett.* **2004**, *14*, 2141−2145.

(18) Byers, L. D. Wolfenden, R. Binding of the by-product analog benzylsuccinic acid by carboxypeptidase A. *Biochemistry* **1973**, *12*, 2070−2078.

(19) Ondetti, M. A.; Condon, M. E.; Reid, J.; Sabo, E. F.; Cheung, H. S.; Cushman, D. W. Design of potent and specific inhibitors of carboxypeptidases A and B. *Biochemistry* **1979**, *18*, 1427−1430.

(20) Ondetti, M. A.; Rubin, B.; Cushman, D. W. Design of specific inhibitors of angiotensin-converting enzyme: New class of orally active antihypertensive agents. *Science* **1977**, *196*, 441−444.

(21) Cushman, D. W.; Ondetti, M. A. Inhibitors of angiotensin-converting enzyme. *Prog. Med. Chem.* **1980**, *17*, 41−104.

(22) Plummer, T. H., Jr.; Ryan, T. J. A potent mercapto bi-product analog inhibitor for human carboxypeptidase N. *Biochem. Biophys. Res. Commun.* **1981**, *98*, 448−454.

(23) Skidgel, R. A. Basic carboxypeptidases: regulators of peptide hormone activity. *TIPS* **1988**, *9*, 299−304.

(24) Huey, R.; Bloor, C. M.; Kawahara, M. S.; Hugli, T. E. Potentiation of the anaphylatoxins *in vivo* using an inhibitor of serum carboxypeptidase N (SCPN). I. Lethality and pathological effects on pulmonary tissue. *Am. J. Pathol.* **1983**, *112*, 48−60.

(25) Lee, K. J.; Joo, K. C.; Kim, E.-J.; Lee, M.; Kim, D. H. A new type of carboxypeptidase A inhibitors designed using an imidazole as a zinc coordinating ligand. *Bioorg. Med. Chem.* **1997**, *5*, 1989−1998.

(26) The numbering system used is the same as that used for the deposited structure 1NSA.

(27) Researchers at Merck have also shown the efficacy of TAFIa inhibition in a model of thrombosis in African green monkeys; see ref 17(a). In addition, researchers at Berlex have recently reported in vivo efficacy data for their TAFIa inhibitor, BX 528; see: Wang, Y.-X.; da Cunha, V.; Vincelette, J.; Zhao, L.; Nagashima, M.; Kawai, K.; Yuan, S.; Emayan, K.; Islam, I.; Hosoya, J.; Sullivan, M. E.; Dole, W. P.; Morser, J.; Buckman, B. O.; Vergona, R. A novel inhibitor of activated thrombin activatable fibrinolysis inhibitor (TAFIa) - Part thrombosis. *Thromb. Haemost.* **2007**, *97*(1), 54−61.

(28) Artursson, P.; Ungell, A.-L.; Löfroth, J. E. Selective paracellular permeability in two models of intestinal absorption: cultured monolayers of human intestinal epithelial cells and rat intestinal segments. *Pharm. Res.* **1993**, *10*, 1123−1129.

(29) He, Y.-L.; Murby, S.; Warhurst, G.; Gifford, L.; Walker, D.; Ayrton, J.; Eastmond, R.; Rowland, M. Species differences in size discrimination in the paracellular pathway reflected by oral bioavailability of polyethylene glycol and D-peptides. *J. Pharm. Sci.* **1998**, *87*, 626−633.

(30) Otwinowski, Z.; Minor, W. Processing of X-ray diffraction data collected in oscillation mode. In *Methods in Enzymology*; Carter, C. W., Jr, Sweet, R. M., Eds.; Academic Press: New York, 1997; Vol. 276, Part A, pp 307−326.

(31) CCP4 suite. *Acta Crystallogr.* **1994**, *D50*, 760−763.

(32) Navaza, J. AMORE. *Acta Crystallogr.* **1994**, *A 50*, 157−163.

(33) Brunger, A. T. Free R value: A novel statistical quantity for assessing the accuracy of crystal structures. *Nature* **1992**, *355*, 472−475.

(34) Laskowski, R. A.; MacArthur, M. W.; Moss, D. S.; Thornton, J. M. PROCHECK: A program to check the stereochemical quality of protein structure. *J. Appl. Crystallogr.* **1993**, *26*, 283−291.

(35) *SMART v5.618* (control) and *SAINT v6.02* (integration) software; Bruker AXS, Inc.: Madison, WI, 1994.

(36) Sheldrick, G. M. *SADABS: Program for Scaling and Correction of Area Detector Data*; University of Göttingen: Göttingen, Germany, 1997 (based on the method of Blessing, R. H. *Acta Cryst.* **1995**, *A51*, 33−38).

(37) Sheldrick, G. M. *SHELXS-97: Program for Crystal Structure Solution*; University of Göttingen: Göttingen, Germany, 1997 (release 97-2).

(38) Sheldrick, G. M. *SHELXL-97: Program for Crystal Structure Refinement*; University of Göttingen: Göttingen, Germany, 1997 (release 97-2).

(39) Flack, H. D. *Acta Cryst.* **1983**, *A39*, 876−881.